Low-field phase diagram of layered superconductors: The role of electromagnetic coupling

Gianni Blatter
Theoretische Physik, Eidgenössische Technische Hochschule Hönggerberg, CH-8093 Zürich, Switzerland

Vadim Geshkenbein and Anatoli Larkin
Theoretische Physik, Eidgenössische Technische Hochschule Hönggerberg, CH-8093 Zürich, Switzerland and L. D. Landau Institute for Theoretical Physics, 117940 Moscow, Russia

Henrik Nordborg
Theoretische Physik, Eidgenössische Technische Hochschule Hönggerberg, CH-8093 Zürich, Switzerland
(Received 14 December 1995)

We determine the position and shape of the melting line in a layered superconductor, emphasizing the importance of electromagnetic interactions in the vortex system. In the limit of vanishing Josephson coupling we obtain a generic reentrant low-field melting line. Finite Josephson coupling pushes the melting line to higher temperatures and fields and a line shape $B_m \propto (1-T/T_c)^{3/2}$ is found. We construct the low-field phase diagram including melting and decoupling lines and discuss various experiments in the light of our results. [S0163-1829(96)02925-6]

Since its proposal in 1988,[1] vortex-lattice melting in bulk type-II material has become a central topic in the phenomenology of high-temperature superconductors. The order, position, and shape of the transition have been investigated theoretically[2] as well as experimentally[3] by a large number of authors. Most recently, the main interest concentrates on the phase diagram of the strongly layered $Bi_2Sr_2Ca_1Cu_2O_8$ (BiSCCO) superconductor which is investigated by means of μSR,[4] neutron scattering,[5] superconducting quantum interference device magnetometry,[6] and Hall-sensor arrays,[7] probing the melting and/or decoupling transition in these materials. The most interesting behavior is found in the low-field part of the phase diagram with $B<1$ kG, where the electromagnetic interactions between the layers becomes relevant, and it is the purpose of this paper to derive and analyze the vortex-lattice melting transition in this regime, taking full account of electromagnetic coupling.

The importance of electromagnetic interactions, adding to the stiffness of individual vortex lines, has been realized before within the context of vortex-lattice melting in the dilute limit,[9] where the transition line exhibits a reentrant behavior (lower branch B_m^l of the melting line, see Fig. 1). As we will show below, the electromagnetic interaction also influences the behavior of the upper branch B_m^u of the low-field melting line and even may change its shape from the usual $B_m(T) \propto (1-T/T_c)^2$ behavior to a new power law $B_m(T) \propto (1-T/T_c)^{3/2}$ within a large part of the phase diagram — this is one of the central results of this paper.

Our analysis below is based on the continuum elastic description of the vortex lattice combined with the Lindemann criterion, stating that the lattice will undergo a melting transition once the mean thermal displacement $\langle u^2\rangle_{\rm th}^{1/2}$ becomes comparable to the lattice spacing $a_o \approx (\Phi_o/B)^{1/2}$, $\langle u^2\rangle_{\rm th}^{1/2}/a_o|_{T_m,B_m} \approx c_L$. The Lindemann number c_L is usually chosen to be a constant of order $c_L \approx 0.1-0.3$. According to Ryu *et al.*,[2] the Lindemann number undergoes some variation in the low-field range discussed here, with c_L changing by a factor 2 while the magnetic field changes by two orders of magnitude.[8] Since only the square (rather than the usual fourth power) of the Lindemann number enters the weak-field result, this drift in c_L is less important. Summarizing, though not rigorous, the Lindemann-type melting scenario has proven very useful and reasonably accurate in predicting the positions of first-order melting transitions in general, and the line shape of the vortex-lattice melting transition in particular.

A well-known limiting case, where strong fluctuations due to dimensional reduction drive a vortex-lattice melting transition, is the superconducting film [two-dimensional (2D) dislocation-mediated Kosterlitz-Thouless melting, see Refs. 10 and 11] and we will begin our analysis with this elementary building block of a layered superconductor. Next, we study a layered system with electromagnetic coupling and derive the shape of the reentrant melting line in this limit. Finally, we account for the Josephson interaction between the layers producing a finite anisotropy parameter $\varepsilon^2 = m/M < 1$, where m and M denote the effective in-plane and c-axis masses. Our results are illustrated in Fig. 1, where we show the shape of the vortex-lattice melting line as it evolves from the 2D isolated layer, to the electromagnetically coupled system of layers, to the Josephson coupled bulk anisotropic superconductor.

Our main task is the calculation of the mean-squared thermal displacement[12]

$$\langle u^2\rangle_{\rm th} \approx \int \frac{d^3k}{(2\pi)^3} \frac{T}{c_{66}K^2 + c_{44}(\mathbf{k})k_z^2}, \tag{1}$$

with the shear modulus c_{66} given by

$$c_{66} = \begin{cases} \sqrt{\dfrac{\pi}{6}}\dfrac{\lambda}{a_o}\dfrac{\varepsilon_o}{\lambda^2}e^{-a_o/\lambda}, & \lambda < a_o, \\ \dfrac{\varepsilon_o}{4a_o^2}, & a_o < \lambda, \end{cases} \tag{2}$$

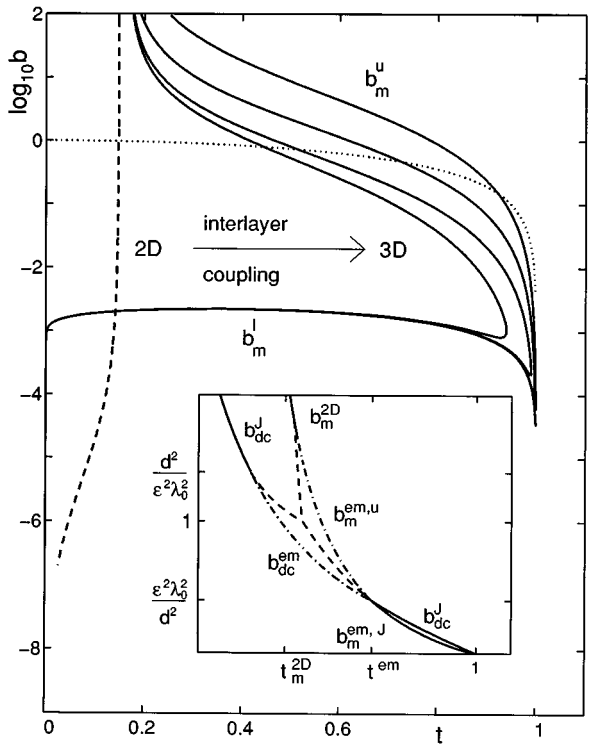

FIG. 1. Low-field phase diagram of a strongly layered superconductor. Reduced units $b=B/(\Phi_o/\lambda_0^2)$ and $t=T/T_c$ have been used ($c_L=0.1$ and parameters appropriate for BiSCCO, see text, have been chosen). The dashed line shows the result for the isolated 2D layer. The solid lines illustrate the 3D bulk results for anisotropy parameters $\varepsilon=0$ (only electromagnetic coupling), $\varepsilon=1/500$, 1/150, and 1/50. The dotted line traces $b(t)=B/[\Phi_o/\lambda^2(t)]$. The inset shows a sketch of the phase diagram comprising melting and decoupling lines. Within our scheme we cannot decide between the dashed ($B_{\rm dc}^{em}$ collapsed onto $B_{\rm dc}^{em,u}$ for $T_m^{2D}<T<T^{em}$) and dash-dotted scenaria for the phase boundaries.

and the dispersive tilt modulus $c_{44}(\mathbf{k})$ consisting of a bulk term $c_{44}^o(\mathbf{k})$ and a single vortex contribution $c_{44}^c(k_z)$, $c_{44}(\mathbf{k})=c_{44}^o(\mathbf{k})+c_{44}^c(k_z)$, with[13]

$$c_{44}^o(\mathbf{k})=\frac{\varepsilon_o}{a_o^2}\frac{4\pi\lambda^2/a_o^2}{1+(\lambda^2/\varepsilon^2)K^2+\lambda^2k_z^2}, \tag{3}$$

$$c_{44}^c(k_z)\approx\frac{\varepsilon_o}{2a_o^2}\left[\varepsilon^2\ln\left(\frac{\lambda^2/\varepsilon^2\xi^2}{1+(\lambda^2/\varepsilon^2)K_{\rm BZ}^2+\lambda^2k_z^2}\right)+\frac{1}{\lambda^2k_z^2}\ln\left(1+\frac{\lambda^2k_z^2}{1+\lambda^2K_{\rm BZ}^2}\right)\right] \tag{4}$$

[in (1) we neglect a second contribution to $\langle u^2\rangle_{\rm th}$ involving lattice compression and keep only the main term]. Here, $\varepsilon_o=(\Phi_o/4\pi\lambda)^2$ denotes the basic energy scale of the continuum elastic theory, $\Phi_o=hc/2e$ is the flux quantum, λ denotes the planar London penetration depth, and ξ is the planar coherence length. The second term in the single vortex tilt c_{44}^c is due to the electromagnetic coupling between the layers, and is the only term in c_{44} surviving the limit $\varepsilon\to0$ (layer decoupling). The electromagnetic contribution to the tilt modulus is strongly dispersive and produces the large stiffness $\varepsilon_l\approx\varepsilon_o/2$ of the vortex lines in the long-wavelength limit $k_z<1/\lambda$. With increasing k_z the electromagnetic stiffness decays $\propto1/\lambda^2k_z^2$ and the line tension crosses over to the well-known result $\varepsilon_l\approx\varepsilon^2\varepsilon_o$ for the anisotropic superconductor as k_z increases beyond $1/\varepsilon\lambda$ (note that this residual tension is due to the Josephson coupling and is relevant only for $\varepsilon\lambda>d$, where d denotes the layer separation). The expression given in (4) is valid for small displacements, in the elastic regime. For large displacements $uk_z>1$ the logarithm in the second term of (4) should be cut on $2\lambda/u$ rather than λk_z.[14] In our analysis below we then replace the logarithm by the factor $\lambda^2k_z^2/(1+\beta\lambda^2k_z^2)$ with $\beta=1/\ln(1+4\lambda^2/c_L^2a_o^2)$, producing a smooth interpolation between the hard and soft tilt modes at large and small wavelengths, respectively.

We start with the analysis of an *individual layer* (we use the definition $\lambda^2/d=\lambda_s^2/d_s$, with λ_s and d_s the penetration depth and thickness of the superconducting layer). In two dimensions a scenario based on the unbinding of dislocation pairs leads to a continuous Kosterlitz-Thouless type melting transition[10,11] at $T_m^{2D}\approx Aa_o^2dc_{66}/2\sqrt{3}\pi$, where the numerical $A\approx0.4-0.75$ accounts for the renormalization of the shear modulus close to the transition. For high fugacities the transition turns first order,[15] and accurate results for the melting temperature are known from Monte Carlo simulations of the 2D Coulomb gas problem; see, e.g., Caillol *et al.*,[16] who find $A\approx0.62$. It is convenient to try reproducing this result within our simple Lindemann approach: dropping the tilt energy in (1), the integral over k_z provides a factor $2\pi/d$ and cutting the K integration on a few lattice spacings we obtain the ratio $\langle u^2\rangle_{\rm th}/a_o^2\approx T\ln\alpha/2\pi c_{66}da_o^2$. Choosing the cutoff parameter $\alpha\approx3$ and a Lindemann number $c_L=(A\ln\alpha/\sqrt{3})^{1/2}/2\pi\approx0.1$ we recover the exact expression for the melting temperature T_m^{2D}. The high-field part ($a_o<\lambda$) of the melting line is field independent,

$$T_m^{2D}\approx\frac{\varepsilon_od}{70}, \tag{5}$$

and using parameters typical for the layered high-T_c superconductors, $T_c\approx100$ K, $\lambda^2(T)\approx\lambda_0^2/(1-T^2/T_c^2)$ with $\lambda_0\approx1800$ Å, and $d=15$ Å, we obtain $\varepsilon_o(T=0)d\approx10^3$ K and $T_m^{2D}\approx15$ K. For a 2D film, the low-field limit ($a_o>\lambda_{\rm eff}=2\lambda^2/d$) of the shear modulus decays algebraically[17] rather than exponentially, $c_{66}\approx0.46\varepsilon_o\lambda_{\rm eff}/a_o^3\propto B^{3/2}$, and we obtain the low-field branch of the 2D melting line in the form (see also Ref. 11)

$$B_m^{2D}\approx\frac{\Phi_o}{\lambda_{\rm eff}^2}\left(\frac{37T}{\varepsilon_od}\right)^2. \tag{6}$$

The result for the melting line of an isolated layer is illustrated in Fig. 1 (dashed line).

Next we consider a finite *electromagnetic coupling* between the layers while keeping $\varepsilon=0$ (no Josephson coupling). In the high-field regime ($a_o<\lambda$) the shear term in (1) dominates over the tilt energy and we recover the field independent 2D result (5). For small fields with $a_o>\lambda$ the tilt energy becomes relevant and the Lindemann criterion reads

$$c_L^2 \approx \frac{2T}{\varepsilon_o d}\frac{\lambda^2}{a_o^2}\left[\frac{1}{4\pi\delta}\ln(1+4\pi\delta\beta)+\frac{d}{\lambda(4\pi\delta)^{1/2}}\right], \quad (7)$$

with $\delta = 2c_{66}\lambda^2/\varepsilon_o$. The first term originates from the soft tilt modes with $k_z\lambda > 1$. The second term involves the long-wavelength modes hardened by the electromagnetic coupling, and becomes relevant only at very small fields $a_o/\lambda > 2\ \ln(\lambda/d)$, where the shear modulus is exponentially small, $\delta \propto \exp(-a_o/\lambda)$. Result (7) provides a lower branch of the melting line which is limited by soft shear and hard tilt,

$$B_m^{em,l}(T) \approx \frac{\Phi_o}{\lambda^2}\frac{1}{4}\left[\ln\left(\frac{4\pi c_L^2}{(3\pi)^{1/4}}\frac{\varepsilon_o\lambda}{T}\right)\right]^{-2}, \quad (8)$$

as well as a tilt limited upper branch

$$B_m^{em,u}(T) \approx \frac{\Phi_o}{\lambda^2}\frac{c_L^2}{2\beta}\frac{\varepsilon_o d}{T} \propto \left(1-\frac{T^2}{T_c^2}\right)^2. \quad (9)$$

The two branches merge near T_c,

$$1-\frac{T_x}{T_c} \approx \frac{\beta G^{2D}}{4c_L^2}\left[\ln\left(\frac{2\pi(2\beta)^{1/2}}{(3\pi)^{1/4}}\frac{c_L}{\sqrt{G^{2D}}}\frac{\lambda_0}{d}\right)\right]^{-2}, \quad (10)$$

and no solid phase can exist at high temperatures beyond T_x. Using typical parameters for the layered high-T_c materials and adopting a value $c_L \approx 0.1$ for the Lindemann number we find T_x close to T_c, $1-T_x/T_c \approx 0.05$ [in (10) we have introduced the 2D Ginzburg number $G^{2D} \approx T_c/\varepsilon_o(T=0)d \approx 0.1$; the logarithms in (8) and (10) take typical values around 5–6]. The reentrant melting line defined by (8) and (9) is illustrated in Fig. 1: The electromagnetic coupling of the layers favors the solid phase and the low-field melting line develops the characteristic ''noselike'' shape of a 3D system. Note that the point of reentrance ends up in the critical region close to T_c. Since our approach accounts for the fluctuations of the phase field via the thermal motion of vortices but neglects amplitude fluctuations of the order parameter, our analysis breaks down in this regime.

In the final step we account for the *Josephson coupling* between the layers producing a finite anisotropy parameter $\varepsilon > 0$. This additional coupling becomes relevant when $a_o, \lambda > d/\varepsilon$ and favors the solid phase, thus pushing the melting line further towards higher temperatures and fields. Evaluating the Lindemann criterion in the low-field regime ($a_o > \lambda$) we recover the previous result (7) with the modification that soft tilt modes are cut on $1/\varepsilon\sqrt{\beta}\lambda$ instead of π/d, leading to the replacement of $\ln(\ldots)/4\pi\delta$ by $(d\sqrt{\beta}/\pi\varepsilon\lambda)[\ln(\ldots)/4\pi\beta\delta + 1]$. The lower branch of the melting line remains unaffected, whereas the upper branch of the low-field melting line takes the form

$$B_m^{em,J}(T) \approx \frac{\Phi_o}{\lambda^2}\frac{\pi c_L^2}{4\sqrt{\beta}}\frac{\varepsilon\varepsilon_o\lambda}{T} \propto \left(1-\frac{T^2}{T_c^2}\right)^{3/2}. \quad (11)$$

The crossing point of the lower and upper branches of the melting line is shifted towards higher temperatures,

$$1-\frac{T_x}{T_c} \approx \frac{1}{2}\left\{\frac{\sqrt{\beta}G^{2D}}{\pi c_L^2}\frac{d}{\varepsilon\lambda_0}\left[\ln\left(\frac{4\sqrt{\beta}}{(3\pi)^{1/4}\varepsilon}\right)\right]^{-2}\right\}^2. \quad (12)$$

For $\varepsilon < d/\lambda_0$ the line $B_m^{em,J}$ goes over into the generic melting line $B_m^{em,u}$ as the temperature drops below $T^{em} \approx T_c[1-\beta(\varepsilon\pi\lambda_0/d)^2]^{1/2}$. For the opposite case, where $\varepsilon > d/\lambda_0$, the generic line $B_m^{em,u}$ is completely hidden, and $B_m^{em,J}$ merges into the well-known bulk anisotropic melting line B_m^J as the field grows beyond Φ_o/λ^2: At these fields the tilt energies are dominated by the dispersive bulk term $c_{44}^o \approx 4\pi\varepsilon^2\varepsilon_o/a_o^4K^2$ [see Eq. (3)], and the Lindemann criterion provides the well-known result

$$B_m^J(T) \approx \frac{\Phi_o}{\lambda^2}4\pi c_L^4\frac{\varepsilon^2\varepsilon_o^2\lambda^2}{T^2} \propto \left(1-\frac{T^2}{T_c^2}\right)^2. \quad (13)$$

At large fields ($a_o < d/\varepsilon < \lambda_0$) the 2D result (5) is recovered.

The most interesting result is the line shape $B_m^{em,J} \sim (1-T/T_c)^{3/2}$, Eq. (11), describing the low-field/high-temperature melting in a Josephson-coupled layered or highly anisotropic superconductor (small parameter $\varepsilon < d/\lambda_0$). This result is due to the electromagnetic coupling which dominates over the bulk-dispersive tilt modulus c_{44}^o as well as over the single-vortex line tension $\varepsilon^2\varepsilon_o$ due to Josephson-coupling in this regime. The substitution of the old result (13) by the new expression (11) is particularly relevant in the strongly layered superconductors such as BiSCCO: The $(1-T/T_c)^{3/2}$ power law is valid provided that $d/\pi\sqrt{\beta}\varepsilon < \lambda < a_o$. Assuming $\varepsilon \sim 1/150$, the second restriction implies $T > 0.4T_c$. In less anisotropic materials, such as YBCO with $\varepsilon \approx 1/5$, this condition is much more stringent and the upper branch of the melting line is always described by the old result, Eq. (13). Note, however, that in YBCO the suppression of the order parameter close to the upper critical field H_{c_2} is relevant and the melting line cannot be described in terms of a simple power law $\propto (1-T/T_c)^2$; see Ref. 2, Blatter and Ivlev, for details (in BiSCCO the melting line is far below H_{c_2} and there is no suppression of the order parameter).

It is instructive to compare the different low-field melting lines as given by Eqs. (9), (11), and (13). A quick inspection gives the ratio $B_m^{em,u}/B_m^J = (d/\lambda\varepsilon c_L)^2 T/8\pi\beta\varepsilon_o d$, which is of order unity taking the above parameters for BiSCCO and using $\varepsilon = 1/150$, a value often quoted in the literature.[4,5] Similarly, $B_m^{em,J}/B_m^J = (d/\lambda\varepsilon c_L)T/16\sqrt{\beta}c_L\varepsilon_o d \approx \alpha[T^2/T_c(T_c-T)]^{1/2}$, where again $\alpha \sim 1$ if we use the above parameters for BiSCCO. The comparison of experimental data for the irreversibility or melting line with the theoretical prediction is often used to extract an estimate for the anisotropy parameter ε, particularly in the strongly layered materials.[4,5] Following up the above discussion we draw attention to an important problem with this procedure: If the anisotropy parameter is very small, say $\varepsilon < 1/500$, the (upper branch of the) low-field melting line (where the comparison theory/experiment is carried out) is dominated by the electromagnetic coupling and no anisotropy parameter can be extracted. The analysis of the melting line can provide a reliable estimate for the anisotropy parameter only if ε is large enough, such that either the bulk result (13) is valid or the mixed electromagnetic/Josephson result (11) can be identified via its particular line shape.

In layered systems an additional thermodynamic transition takes the 3D bulk system into a system of decoupled 2D

layers.[13] The loss of interlayer coherence is due to strong thermal fluctuations of the pancake vortices within the individual layers, and the transition line can be estimated within a Lindemann-type approach: decoupling occurs when the interlayer phase correlator

$$\langle(\delta\varphi)^2\rangle \sim \frac{T}{d a_o^4}\int \frac{d^2K}{K^2}\,\frac{1}{c_{66}K^2+c_{44}d^{-2}} \tag{14}$$

becomes of order unity. The conventional analysis based on an intermediate anisotropy with $\varepsilon > d/\lambda_0$ predicts a high-field decoupling line in the solid at low temperatures $T<T_m^{2D}$ and a low-field decoupling line in the liquid for $T>T_m^{2D}$ [with $c_{66}=0$ in (14)]. The shape follows from the above criterion and takes the form $B_{dc}^J \approx (\Phi_o \varepsilon^2/d^2)(\varepsilon_o d/70T)^n$, with $n=2\,(1)$ at low (high) temperatures. The situation changes when the anisotropy is large, $\varepsilon < d/\lambda_0$. For fields $B<\Phi_o d^2/\varepsilon^2\lambda^4$ the decoupling line takes the form $B_{dc}^{em}\approx(\Phi_o/\lambda^2)(\varepsilon_o d/70T)$ (see also Ref. 18). Within the intermediate temperature regime $T_m^{2D}<T<T^{em}$ this expression coincides (up to a numerical factor of order unity) with the one for the melting line $B_m^{em,u}$, see Eq. (9). At high temperatures $T>T^{em}$ decoupling occurs in the liquid phase following B_{dc}^J as given above. Whether the decoupling line collapses with the melting line in the intermediate regime $T_m^{2D}<T<T^{em}$ or marks a separate transition *below* the melting line cannot be decided on the basis of the above arguments. In both cases, however, the resulting phase diagram (see inset of Fig. 1) looks markedly different from that predicted by the previous analyses.

Recently, a first-order phase transition has been observed in the low-field ($B<\Phi_o/\lambda^2$) regime of a strongly layered BiSCCO superconductor.[7] The jump in the magnetization observed at the transition can be associated either with a vortex-lattice melting- or with a layer-decoupling transition. Fits using a $(1-T/T_c)^{1.55}$ (melting) or a $(T_c/T-1)$ (decoupling) power-law behavior produce a satisfactory agreement with the data over most of the measured temperature interval.[7] Our result (11) then is in good agreement with the measured power-law behavior based on the melting scenario. Whether the observed transition indeed can be attributed to a first-order melting transition remains to be shown, however.

In conclusion, we have presented Lindemann-based estimates for the position and shape of the melting line in a layered superconductor, accounting for the electromagnetic interaction between vortices. Results for the melting line have been obtained in the low-field regime $B<\Phi_o/\lambda^2$: In the absence of Josephson coupling between the layers we have found a generic reentrant melting line independent of the material anisotropy. Including a finite Josephson coupling, the upper branch of the melting line is pushed out to higher temperatures and fields and takes on a characteristic line shape $\propto(1-T/T_c)^{3/2}$. We have discussed the influence of electromagnetic interactions on the decoupling line, and have drawn attention to the quantitative and possible qualitative changes in the low-field phase diagram of layered superconductors.

We thank E. H. Brandt for helpful discussions, and the Swiss National Foundation for financial support.

[1] D. R. Nelson, Phys. Rev. Lett. **60**, 1973 (1988).
[2] E. Brézin *et al.*, Phys. Rev. B **31**, 7124 (1985); A. Houghton *et al.*, *ibid.* **40**, 6763 (1989); E. H. Brandt, Phys. Rev. Lett. **63**, 1106 (1989); S. Sengupta *et al.*, *ibid.* **67**, 3444 (1991); S. Ryu *et al.*, *ibid.* **68**, 710 (1992); G. Blatter and B. Ivlev, Phys. Rev. B **50**, 10 272 (1994).
[3] D. Farrell *et al.*, Phys. Rev. Lett. **67**, 1165 (1991); A. Schilling *et al.*, Phys. Rev. B **46**, 14 253 (1992); H. Safar *et al.*, Phys. Rev. Lett. **69**, 824 (1992); W. Kwok *et al.*, *ibid.* **72**, 1092 (1994).
[4] S. Lee *et al.*, Phys. Rev. Lett. **71**, 3862 (1993).
[5] R. Cubitt *et al.*, Nature (London) **365**, 407 (1993).
[6] H. Pastoriza *et al.*, Phys. Rev. Lett. **72**, 2951 (1994).
[7] E. Zeldov *et al.*, Nature (London) **375**, 373 (1995).
[8] Note that the simulations by Ryu *et al.*, Ref. 2, do not account for electromagnetic coupling and treat Josephson coupling only in an approximate way; it remains unclear in as far this simulation can be used for an estimate of c_L.
[9] D. Fisher *et al.*, Phys. Rev. B **43**, 130 (1991).
[10] B. Halperin and D. Nelson, Phys. Rev. Lett. **41**, 121 (1978); B. Huberman and S. Doniach, *ibid.* **43**, 950 (1979).
[11] D. Fisher, Phys. Rev. B **22**, 1190 (1980); D. Fisher *et al.*, *ibid.* **20**, 4692 (1979).
[12] G. Blatter *et al.*, Rev. Mod. Phys. **66**, 1125 (1994).
[13] L. Glazman and A. Koshelev, Phys. Rev. B **43**, 2835 (1991).
[14] J. Clem, Phys. Rev. B **43**, 7837 (1991).
[15] A. Jonsson *et al.*, Phys. Rev. Lett. **70**, 1327 (1993).
[16] J. Caillol *et al.*, J. Stat. Phys. **28**, 325 (1982).
[17] E. Conen and A. Schmid, J. Low Temp. Phys. **17**, 331 (1974).
[18] L. Daemen *et al.*, Phys. Rev. B **47**, 11 291 (1993).